Density Functional Calculations on Model Tyrosyl Radicals

F. Himo,* A. Gräslund,# and L. A. Eriksson*
*Department of Physics, and #Department of Biophysics, Arrhenius Laboratories, Stockholm University, Stockholm, Sweden

ABSTRACT A gradient-corrected density functional theory approach (PWP86) has been applied, together with large basis sets (IGLO-III), to investigate the structure and hyperfine properties of model tyrosyl free radicals. In nature, these radicals are observed in, e.g., the charge transfer pathways in photosystem II (PSII) and in ribonucleotide reductases (RNRs). By comparing spin density distributions and proton hyperfine couplings with experimental data, it is confirmed that the tyrosyl radicals present in the proteins are neutral. It is shown that hydrogen bonding to the phenoxyl oxygen atom, when present, causes a reduction in spin density on O and a corresponding increase on C_4. Calculated proton hyperfine coupling constants for the β-protons show that the α-carbon is rotated 75–80° out of the plane of the ring in PSII and *Salmonella typhimurium* RNR, but only 20–30° in, e.g., *Escherichia coli*, mouse, herpes simplex, and bacteriophage T4-induced RNRs. Furthermore, based on the present calculations, we have revised the empirical parameters used in the experimental determination of the oxygen spin density in the tyrosyl radical in *E. coli* RNR and of the ring carbon spin densities, from measured hyperfine coupling constants.

INTRODUCTION

There is now a growing body of experimental evidence for the existence of both stable and transient amino acid radicals in the electron transfer pathways in, e.g., photosystem II (PSII) in green plants or ribonucleotide reductases (RNRs) in bacteria or higher organisms. Through electron spin resonance spectroscopy (ESR), electron nuclear double-resonance measurements (ENDOR), electron spin echo envelope measurements (ESEEM), and x-ray crystallography, the positions and properties of some of these species have been carefully determined (Barry et al., 1990; Bender et al., 1989; Gräslund and Sahlin, 1996, and references therein; Hoganson and Babcock, 1992; Hoganson et al., 1996; Nordlund and Eklund, 1993; Nordlund et al., 1990; Rigby et al., 1994; Sahlin et al., 1982; Tommos et al., 1995; Warncke et al., 1994). Many unknowns still prevail, however, regarding, e.g., the influence of hydrogen bonding, the exact local geometries, and, in some cases, whether the species exist as neutral radicals (through the removal of a hydrogen atom) or as radical cations (in which only an electron has been removed, but where the proton remains bound to the amino acid side chain). It has been proposed by Barry and Babcock (1987) that accurate *g*-tensor analyses can be employed to distinguish between neutral and cationic radicals.

One such intriguing amino acid radical system is the oxidized deprotonated tyrosyl radical, shown to participate in the charge transfer pathways of several biological systems. In RNR and PSII, the tyrosyl side chain is located in the vicinity of a transition metal with redox activity that is essential for biological function (Nordlund and Eklund, 1993). Also present in the hydrophobic cavity surrounding the tyrosyl group are some aspartate and histidine groups, allowing for further stabilization through hydrogen bonding, and in some cases participating in subsequent steps of the charge transport (Gräslund and Sahlin, 1996, and references therein; Nordlund and Eklund, 1993; Nordlund et al., 1990).

Parallel to the latest breakthroughs in the experimental detection of these types of systems, theory has now reached the state where it actively can contribute detailed knowledge to solving many of the problems of interest in biophysics. With this aspect in mind, we have recently started to investigate the properties of the amino acid radicals involved in the above-mentioned charge transfer processes from a theoretical perspective. In the present work we concentrate on the tyrosyl radical and show this to be a novel case where the high precision of recently determined experimental spin densities (Hoganson et al., 1996) is perfectly matched by that of the theoretical methodology based on gradient-corrected density functional theory (DFT).

DFT has evolved over the last five years into one of the major approaches in computational quantum chemistry and has been shown in a number of studies to yield geometric structures within 0.01 Å and 1–2°, binding energies within a few kcal/mol, and—of particular interest in the present study—radical hyperfine couplings generally within ~20% of experimental data (Andzelm and Wimmer, 1992; Johnson et al., 1993; Bauschlicher, 1995; Malkin et al., 1995, and references therein; Barone, 1994, 1996; Cohen and Chong, 1995). DFT, furthermore, has the computational advantage that we are able to treat far larger systems than with conventional Hartree-Fock-based ab initio methods, because of a favorable scaling with increasing number of electrons, with a retained high level of accuracy.

Received for publication 3 September 1996 and in final form 13 December 1996.

Address reprint requests to Dr. Leif A. Eriksson, Department of Physics, Stockholm University, Box 6730, S-113 85 Stockholm, Sweden. Tel.: 46-8-164616; Fax: 46-8-347817; E-mail: leifaxel@physto.se

0006-3495/97/04/1556/12 $2.00

THEORETICAL METHOD

The gradient-corrected DFT functionals developed by Perdew and Wang for the exchange term (PW) (Perdew and Wang, 1986) and by Perdew for the correlation contribution (P86) (Perdew, 1986a,b) have been employed throughout the study. This functional combination has previously proved (together with the "B3LYP" hybrid functional; Becke, 1993; Lee et al., 1988) to be the most appropriate form for studies of radical hyperfine properties, routinely generating hyperfine coupling constants (hfcc) within 20% of experimental values for a wide range of radical systems (Malkin et al., 1995, and references therein; Barone, 1994, 1996; Eriksson et al., 1994, 1995; Eriksson, 1995), provided basis sets of sufficient accuracy are employed. (The form implemented and used for hfcc calculations does, however, differ slightly from the original suggestion by Becke.) Problem cases do exist, however, where the deviations are far larger.

The orbital basis sets employed for the hyperfine structure calculations belong to the IGLO-III family (Kutzelnigg et al., 1990) (IGLO: individual gauge of localized orbitals). These are based on Huzinaga's 11s7p series (Huzinaga, 1965; Huzinaga and Sakai, 1969), which are very loosely contracted and to which a double set of polarization functions are added. To increase computational speed, the geometries were optimized throughout by using the smaller local density-optimized double zeta plus valence polarization (DZVP) bases by Andzelm and co-workers (Godbout et al., 1992), followed by single-point hfcc calculations using the larger IGLO bases. Initial tests showed that although the DZVP basis yielded slightly longer bonds than IGLO-III (~0.1 Å), the spin densities and hfcc were almost identical between the IGLO-III//DZVP and the IGLO-III//IGLO-III calculations. For the fitting of the charge density and the approximate exchange-correlation potential, we have used the auxiliary basis sets (5, 1;5, 1) for H and (5, 2;5, 2) for the remaining atoms (Sim et al., 1991). The digits denote the number of s, spd even-tempered Gaussian functions used in the fitting procedures. The deMon program is used throughout (St-Amant and Salahub, 1990; St-Amant, 1991; Salahub et al., 1991; Daul et al., 1993).

The hyperfine coupling constants are part of the spin Hamiltonian and arise from the interaction between the unpaired electron(s) and the magnetic nuclei in the sample. The isotropic component of the 3×3 hyperfine interaction tensor is related to the spin density at the positions of the nuclei, and can be computed using the expression

$$A_{\mathrm{iso,N}} = \frac{4\pi}{3} g_e \beta_e g_N \beta_N \langle S_z \rangle^{-1} \sum_{\mu,\nu} P_{\mu,\nu}^{\alpha-\beta} \langle \phi_\mu(\vec{r}_{kN}) | \delta(r_{kN}) | \phi_\nu(\vec{r}_{kN}) \rangle.$$

In the equation, $P_{\mu,\nu}^{\alpha-\beta}$ is an element of the spin density matrix; g_e and β_e are the electronic g-factor (taken as the free electron value, 2.0023) and Bohr magneton, respectively; g_N and β_N are the corresponding nuclear terms; and $\langle S_z \rangle$ is the value of the spin angular momentum (1/2 for doublet systems). The Dirac delta function ensures that the integral is evaluated at the position of the nuclei only.

The remainder of the hyperfine tensor, once the isotropic component has been subtracted out, is referred to as the anisotropic, or dipolar, hyperfine part. This is obtained by using integrals describing dipole-dipole interactions, multiplied by essentially the same prefactors as shown above. The exact formulae for computing radical hfcc have been given in great detail elsewhere (cf. Malkin et al., 1995, and references therein). The total spin densities, also reported in the present work, were obtained throughout by Mulliken population analysis.

RESULTS AND DISCUSSION

Choice of model for the tyrosyl radical and radical cation

The unpaired electron in the tyrosine radical or radical cation will be localized almost entirely to the phenoxyl ring of the side chain (Barry et al., 1990; Bender et al., 1989; Gräslund and Sahlin, 1996, and references therein; Hoganson and Babcock, 1992; Rigby et al., 1994; Sahlin et al., 1982; Tommos et al., 1995; Warncke et al., 1994). Hence from a computational perspective, it is of primary interest to find a model that closely describes all of the features of the system as observed experimentally, but in which we can neglect as far as possible the main part of the protein backbone. To this end, three systems of increasing size have been employed to approximate the neutral tyrosyl radical: phenoxyl (C_6H_5O), *p*-methylphenoxyl ($CH_3C_6H_4O$), and *p*-ethylphenoxyl ($CH_3CH_2C_6H_4O$) (Fig. 1 *a–c*, respectively). For the corresponding radical cations, we used the smallest model only, $C_6H_5OH^+$ (Fig. 1 *d*).

The PWP86/DZVP optimized geometries of these four systems are displayed in Fig. 1, and in Table 1 we list the total atomic spin densities computed at the PWP86/IGLO-III level on these geometries. In the table we also include some experimental data observed for the tyrosyl radicals in a few different proteins (Hoganson et al., 1996; Tommos et al., 1995), and previous theoretical values obtained at the density functional theory B3LYP/6-31G(d) and SVWN/6-31G(d) levels and the semiempirical AM1/INDO level (Qin and Wheeler, 1995a, 1996; O'Malley et al., 1995). The optimized structure of the smallest phenoxyl radical and the radical cation agrees very closely with those obtained at, in particular, the BLYP/6-31G(d) level by Qin and Wheeler (1995b, 1996). In comparison with data from calculations at correlated ab initio and various other DFT levels (Chipman et al., 1994; Liu and Zhou, 1993; Qin and Wheeler, 1995b, 1996), the PWP86/DZVP optimized bond lengths are slightly longer—which is similar to the observation made between the structures obtained with the DZVP and IGLO-III bases described above. Substituting the hydrogen bonded to C_1 (in *para* position to the oxygen) for a methyl or ethyl group (Fig. 1, *b* and *c*, respectively) has essentially no effect

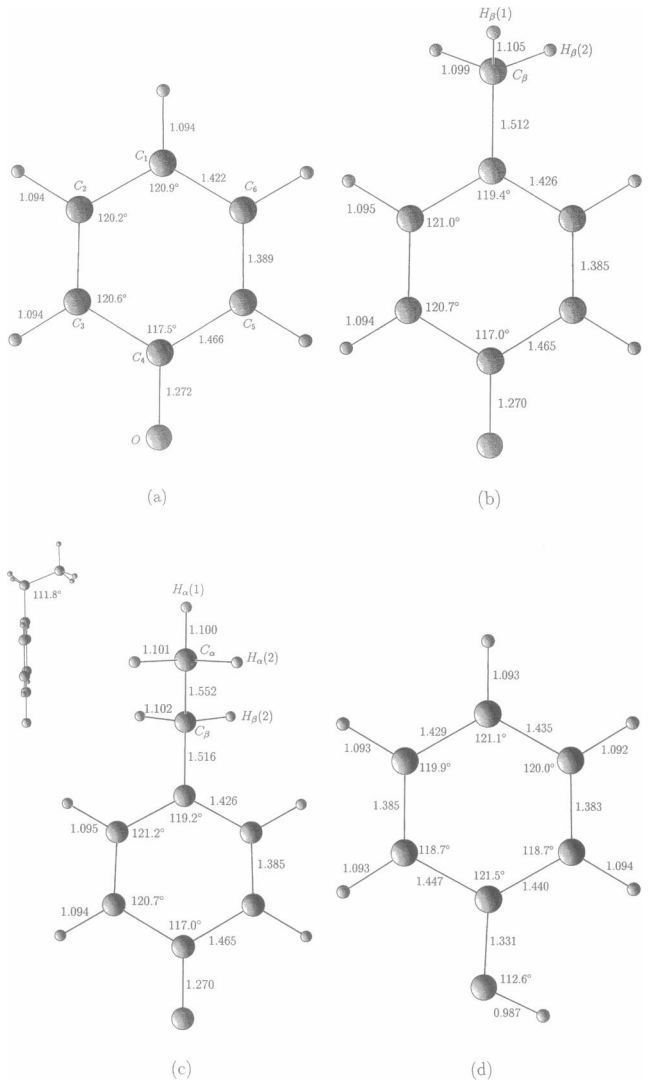

FIGURE 1 PWP86/DZVP optimized geometries of the four tyrosyl radical/radical cation models used in the study. Absolute energies obtained from single-point PWP86/IGLO-III calculations on the optimized structures are (*a*) phenoxyl radical, −307.33260 a.u.; (*b*) *p*-methylphenoxyl radical, −346.71936 a.u.; (*c*) *p*-ethylphenoxyl radical, −386.09989 a.u.; and (*d*) phenoxy radical cation, −307.67125 a.u., respectively.

on the geometry of the remainder of the system, in agreement with earlier findings (Qin and Wheeler, 1995a). For the ethyl-substituted species, two models differing in the relative orientation of the ethyl tail (rotation about the C_1-Cβ bond) were investigated. To retain a plane of symmetry in the system we placed the ethyl group carbon atoms either in the benzene ring plane or perpendicular to this. The C_α-C_β-C_1-C_6 dihedral angles in these two models are defined as 0° (in plane) or 90° (out of plane), respectively. The conformation of lowest energy was found when the α-carbon was locked perpendicular to the ring plane, as displayed in Fig. 1 *c*. As expected, the geometric differences between the phenoxyl radical (Fig. 1 *a*) and the protonated radical cation (Fig. 1 *d*) are much larger than what we observe by alkyl substition to the neutral system. In particular, the C_4-O bond is found to increase significantly, from 1.272 Å to 1.331 Å.

The total atomic spin densitites, obtained from Mulliken population analysis, clearly display the alternating pattern expected for these types of systems (Table 1). The spin density is entirely localized to the ring carbons and the oxygen, also for the alkyl-subtituted systems 1 *b* and 1 *c*. All hydrogen spin densities are less than 0.03 a.u. for all systems, and thus are not included in the table. Comparing the present spin densities with experimental data (Hoganson et al., 1996; Tommos et al., 1995), we find that there is a close agreement with the data obtained for the neutral systems, although the computed oxygen spin densities appear to be overestimated. The reason for this is either a significant, localized cation character of the oxygen end (as the agreement with the remaining atoms in the neutral systems is most satisfactory), or that the empirically based experimental estimates of the oxygen spin density are incorrect. Both of these aspects are investigated in detail below. Because atomic spin densities are realtively insensitive to the level of theory, the PWP86/IGLO-III data are in good agreement with the DFT data reported by Qin and Wheeler (1995a, 1996). In accordance with the currently observed effects of alkyl substitution of the neutral system, Qin and Wheeler also found that adding the full amino acid backbone to the system has little effect on the spin densities on the phenoxyl fragment (Qin and Wheeler, 1995a). We also note that their LDA spin densities for neutral phenoxyl appear to be closer to experiment than do the present PWP86/IGLO-III results. This is most likely caused by the use of an insufficient method in the previous work, as it is a well-known artefact of the LDA method to generate a too small localization of the electron density. From a theoretical standpoint, the present approach is more accurate. Qin and Wheeler did not report spin densities from their more recent (and more accurate) B3LYP/6-31G(d) studies (Qin and Wheeler, 1996). The spin densities on oxygen and three of the carbons (C_3-C_5) in the cationic system deviate considerably from those of the neutral systems (Table 1).

In Table 2 we show the PWP86/IGLO-III//DZVP computed hyperfine coupling constants (^{1}H, ^{13}C, and ^{17}O) for systems 1 *a* and 1 *d*, and in Table 3 we summarize the experimental data available for the ring protons. Previous theoretical data include empirical estimates using the relations by Stone and Maki (1962) for the rotation of the alkyl chain and the McConnell-Strathdee relations (McConnell and Strathdee, 1959, and references therein) for the ring protons, calculations using the semiempirical AM1/INDO approaches on the neutral systems (Allard et al., 1996; Barry et al., 1990; Bender et al., 1989; Hoganson and Babcock, 1992; O'Malley et al., 1995; Rigby et al., 1994), and, very recently, DFT computed isotropic proton hfcc for the cation (Qin and Wheeler, 1996). In Table 2 we have listed the hyperfine couplings as A_{iso}, T_{xx}, and T_{zz}. These are converted to the experimentally measured values (Table 3) by adding the isotropic component to the anisotropic ones (i.e., $A_{ii} = A_{iso} + T_{ii}$).

TABLE 1 Atomic spin densities on carbon and oxygen in the four tyrosyl model systems shown in Fig. 1

Atom	Fig. 1 *a* (neutral)	Fig. 1 *b* (neutral)	Fig. 1 *c* (neutral)	Fig. 1 *d* (cation)	*E. coli* RNR	Spinach Y_D PSII	SVWN/ 6-31G(d) (neutral)	AM1 (neutral)	B3LYP/ 6-31G(d) (cation)
C1	0.40	0.39	0.39	0.43	0.38	0.37	0.32	0.33	0.46
C2	−0.13	−0.12	−0.12	−0.06	−0.08	−0.07	−0.06	0	−0.10
C3	0.30	0.28	0.28	0.17	0.25	0.24	0.24	0.22	0.18
C4	−0.05	−0.03	−0.03	0.21	−0.05	0.01	−0.02	0.04	0.22
C5	0.30	0.28	0.28	0.14	0.25	0.24	0.24	0.23	0.12
C6	−0.13	−0.12	−0.12	−0.03	−0.08	−0.07	−0.06	0	−0.05
O	0.38	0.36	0.37	0.20	0.29	0.26	0.38	0.17	0.19
C_β	—	−0.04	−0.04	—	0.03	0.01	—	—	—
C_α	—	—	0.03	—	—	—	—	—	—

a, *b*, *c*, Neutral radicals; *d*, radical cation. Experimental data for neutral tyrosyl free radicals in spinach PSII Y_D and *E. coli* RNR (Hoganson et al., 1996; Tommos et al., 1995), and computed data for the phenoxyl radical (SVWN/6-31G(d) (Qin and Wheeler, 1995a) and AM1 (O'Malley et al., 1995)), and the phenol radical cation (B3LYP/6-31G(d) (Qin and Wheeler, 1996)) are also included for comparison.

Similar to the results for the spin densities, the hfcc of the different neutral systems show only small variations due to the alkyl substitution, whereas the data for the cationic system deviate considerably from those obtained for the neutral ones. With the one exception of the C_1 carbon in the methyl-substituted radical (Fig. 1 *b*), the changes between the hfcc of the neutral models are in most cases within 0.5 G. In the ethyl-substituted compound (Fig. 1 *c*; not included in the table), isotropic ^{13}C hfcc of 11.2 G (C_α) and −3.7 G (C_β) are obtained in the case where the α-carbon lies perdendicular to the plane of the benzene ring. The anisotropies are very small throughout.

Experimental data are available for the hydrogens in the phenoxyl and *p*-methylphenoxyl radicals and the phenol radical cation. Comparing computed isotropic proton hfcc of the two neutral radicals with experiment (Table 2), we note that the H2/H6 protons are in very close accord, but that the H3/H5 protons are ~0.5 G too small. The experimental decrease in hfcc on H3/H5 upon methyl substitution (0.4–0.5 G) is, however, well described. For the methyl group, comparison between the computed averaged results and the rotationally averaged data observed experimentally should be made with some caution, as we have not made a full averaging including the rotational motion in the present work, but have merely summed the static contributions from the three protons at the global potential energy minimum. For the cation radical, the deviation between theory and experiment is slightly larger. A comparison with the calculated B3LYP/6-31G(d) hfcc of the phenol radical cation also displays some deviations. The agreement of the present work with experiment is better for H2/H6 but worse for H1 and H3/H5. Because of the considerable difference in the

TABLE 2 PWP86/IGLO-III//DZVP calculated hyperfine coupling constants (Gauss) for ^1H, ^{13}C, and ^{17}O isotopes in the phenoxyl radical (Fig. 1 *a*), the *p*-methylphenoxyl radical (Fig. 1 *b*), and the phenoxy radical cation (Fig. 1 *d*).*

Atom	Phenoxyl radical			*p*-Methylphenoxyl radical			Phenoxy radical cation		
	A_{iso}	T_{xx}	T_{zz}	A_{iso}	T_{xx}	T_{zz}	A_{iso}	T_{xx}	T_{zz}
C1	12.01	−10.68	20.73	12.05	−10.78	20.95	13.04	−12.38	24.31
C2	−8.08	−4.70	2.62	−7.43	−4.06	2.27	−6.02	−1.98	1.17
C3	7.39	−7.71	15.08	6.70	−7.27	14.18	2.97	−5.15	9.88
C4	−10.08	−1.35	1.66	−9.46	−0.77	1.39	2.53	−7.56	14.85
C5	7.39	−7.71	15.08	6.70	−7.27	14.18	1.33	−3.93	7.47
C6	−8.08	−4.70	2.62	−7.43	−4.06	2.27	−4.82	−0.35	0.29
O	−7.68	−41.16	20.63	−7.36	−39.47	19.78	−5.51	−24.34	12.43
H1	−8.03	−5.28	5.48	—	—	—	−9.52	−5.89	6.55
H2	1.81	−1.02	1.00	1.46	−1.03	0.95	0.48	−1.02	1.43
H3	−6.01	−3.16	3.97	−5.66	−3.02	3.79	−4.17	−2.45	3.46
H5	−6.01	−3.16	3.97	−5.66	−3.02	3.79	−3.28	−2.04	3.02
H6	1.81	−1.02	1.00	1.46	−1.03	0.95	−0.21	−0.97	1.78
H_o	—	—	—	—	—	—	−4.34	−4.89	7.34
C_β	—	—	—	−4.55	−0.47	0.53	—	—	—
$H_\beta(3)$	—	—	—	10.80	−0.78	1.27	—	—	—

The T_{yy} components are obtained using the zero trace condition of the dipolar tensor ($T_{xx} + T_{yy} + T_{zz} = 0$).

*Experimentally determined isotropic proton couplings are for the phenoxyl radical: H1, 10.2; H2/H6, 1.9; H3/H5, 6.6 G, respectively (Neta and Fessenden, 1974). Same data for the *p*-methylphenoxyl radical are H2/H6, 1.4; H3/H5, 6.1; and $H_\beta(3)$, 12.3 G (Dixon and Norman, 1964). For the phenol radical cation, experimental couplings are H1, 10.7; H2/H6, 0.8; H3/H5, 5.3 G (Dixon and Murphy, 1972), and calculated at the B3LYP/6-31G(d) level, H1, −11.1; H2/H6, 1.3/0.1; H3/H5, −5.2/−3.9 G (Qin and Wheeler, 1996).

TABLE 3 Experimental proton hfcc (Gauss) for the ring protons in the tyrosyl radical reported in various proteins, and for the *p*-methylphenoxyl radical

System	H2/H6			H3/H5		
	A_{xx}	A_{yy}	A_{zz}	A_{xx}	A_{yy}	A_{zz}
C_6H_5O (calc.)	0.79	1.83	2.81	−9.17	−6.82	−2.04
p-CH_3-C_6H_5O (calc.)	0.43	1.55	2.41	−8.68	−6.43	−1.87
p-CH_3CH_2-C_6H_5O* (calc.)	0.46	1.58	2.43	−8.83	−6.56	−1.98
$C_6H_5OH^+$ (calc.)	−0.86	−0.48	1.74	−5.97	−4.73	−0.49
Spinach Y_Z, PSII#	0.5	1.8	2.7	−9.5	−6.9	−3.0
Spinach Y_D, PSII§	—	1.7	2.5	−9.1	−6.8	−2.8
E. coli RNR¶	—	1.7	2.7	−9.6	−7.0	−2.8
S. typhim. RNR‖	—	—	—	−11.5	−7.1	−2.5
p-Methylphenoxyl radical**	0.8	1.7	2.55	9.75	6.5	3.25

For comparison, we also include the calculated values for the phenoxyl radicals, and the phenoxy radical cation (cf. Fig. 1), converted to the A_{xx}, A_{yy}, A_{zz} format. For the cation, the H2/H6 and the H3/H5 protons are unequivalent (because of the presence of the oxygen-bonded proton). Hence there we have taken the average values for each component.

*90° rotational angle.

#Tommos et al., 1995.

§Rigby et al., 1994.

¶Bender et al., 1989.

‖Allard et al., 1996.

**Babcock et al., 1992.

accuracy of the basis sets employed in the two studies, however, firm conclusions cannot be made from this limited data set.

Using the full hyperfine tensor (A_{xx}, A_{yy}, A_{zz}), the computed values for the *p*-ethylphenoxyl radical (Fig. 1 *c*) are (0.5, 1.6, 2.4) G for H2/H6 and (−8.8, −6.6, −2.0) G for H3/H5, in very close agreement with, e.g., the EPR data by Tommos et al. (1995), recorded for the Y_z tyrosyl radical in PSII: (0.5, 1.8, 2.7) G for H2/H6 and (−9.5, −6.9, −3.0) G for H3/H5. For the radical cation, the corresponding averaged values are (−0.9, −0.5, 1.7) G for H2/H6 and (−6.0, −4.7, −0.5) G for H3/H5, respectively, in poor agreement with the data observed for the biological systems.

In a study by Bender et al. (1989), the proportionality constant in the McConnell equation for hydrogens bonded to a phenol ring was derived as $A_{iso}(H_n) = Q \times \rho(C_n)$, Q = (−)24.9 G. From the present work, using the PWP86/IGLO-III computed values of $A_{iso}(H_n)$ and adjacent total carbon atom spin density $\rho(C_n)$ on all four systems, we obtain distinctively different values for the H2/H6 protons compared to the H3/H5 protons. For the former $Q = -13 \pm 2$ G, and for the latter $Q = -22 \pm 2$ G (because of the very small spin densities on C2/C6 and corresponding proton couplings for the cation, these particular nuclei display some irregularities in the pattern). Hence we note that for H3/H5, the empirical estimate by Bender et al. agrees well, whereas for the two protons furthest away from the oxygen atom, the Q value is only about half of the empirical value. There is no obvious explanation for this phenomenon. It might be related to the numerically small and negative spin densities on C_2 and C_6, where the McConnell relation may not be entirely valid. Another explanation could be made in terms of an overestimation of the present approach of the alternating character of the spin density. As the hydrogen hyperfine couplings are accurately computed, a too large numerical value of $\rho(C)$ would render a Q value that is too small. Further studies are needed to elucidate this aspect.

In a very recent work by Hoganson et al. (1996), ^{17}O data were recorded for the tyrosyl radical in *E. coli* RNR. The A_{zz} component (A_{xx} in our orientation of the coordinate system) was determined to be −44.9 G. This agrees well with our values of −48.8 G for the phenoxyl radical, −46.8 G for *p*-methylphenoxyl, and −47.0 G for *p*-ethylphenoxyl. For the radical cation the value is far too small (−30.0 G), providing further evidence that the tyrosyl radical observed in these biological systems is, in fact, neutral.

Using experimental EPR data from studies of peroxide radicals, ROO$^\bullet$ (Sevilla et al., 1990; Broze et al., 1967) and the empirical McConnell-Strathdee relations (McConnell and Strathdee, 1959, and references therein), the A_{xx} and A_{yy} components and the spin density were then derived by Hoganson for the tyrosyl oxygen. The estimated values for the *xx* and *yy* components of the hyperfine tensor are quite low, however (+4.9 G, compared with our calculated values of +13 G), as is the experimental oxygen spin density (exp.: 0.29, calc.: 0.37). Based on previous experience (Eriksson et al., 1994, 1995; Eriksson, 1995; Barone, 1996), the calculated values for the anisotropic components of the hyperfine tensor are generally correct to within 10% for systems of this type, whereas values for the isotropic components computed at this level of theory might deviate by 10–20%. Hence it seems highly unlikely that the calculations would generate errors as large as those we see in this case.

To investigate in more detail the source of this discrepancy between theory and experimental estimates, we computed the hfcc for a subset of the peroxide systems on which the empirical parameterization for the oxygen hf tensor in the tyrosyl radical was based. The same approach was used as for the tyrosines in this work (PWP86/DZVP optimizations followed by PWP86/IGLO-III single-point ESR cal-

culations). The agreement with experimental data was found to lie within a few percent for both the peroxide oxygens, for all systems investigated (Himo and Eriksson, to be published). We can therefore assume that the theoretical approach used is flexible enough to accurately describe the different chemical environments found in peroxide and oxo radicals. The reason for the discrepancy between calculated and estimated values for ^{17}O may instead be found in the use of empirical parameters determined for a chemically quite different type of atom. The empirical McConnell rules relating hyperfine couplings to spin densities are, in this case,

$$A_{iso} = Q \cdot \rho(O),$$

$$A_{xx} = A_{yy} = (Q - B) \cdot \rho(O)$$

and

$$A_{zz} = (Q + 2B) \cdot \rho(O).$$

In the experimental studies of peroxide systems, the values $Q = -40$ G/a.u. and $B = -57$ G/a.u. were determined (Sevilla et al., 1990; Broze et al., 1967). These values were then used together with the experimental A_{zz} value to determine $\rho(O)$ in the tyrosyl radical in *E. coli* RNR (Hoganson et al., 1996). Using the same relations together with our calculated data for the hyperfine couplings and the total oxygen spin density instead yields a revised set of parameters as $Q = -20.5$ G and $B = -54.6$ G. If we then redo the derivation of the oxygen spin density using these new parameters together with the experimental A_{zz} value of -44.7 G (Hoganson et al., 1996), we obtain $\rho(O) = 0.35$. This is in much closer agreement with the computed value of 0.37 ± 0.01 for our three model systems. From this we may conclude that the empirical relations between spin density and hyperfine couplings work well, but that the empirical parameters (in particular, the isotropic Q value) must be chosen with great care. The reason for the originally observed difference between experiment and theory for both the derived hf tensor components and the spin density on oxygen is thus most likely related to inappropriate empirical parameters, rather than to a local cationic character of the oxygen.

Effects of ethyl group rotation

For the ethyl-substituted system (Fig. 1 *c*) we may compare theoretical and experimental hfcc for the β-protons, located on the carbon closest to the benzene ring. The hyperfine couplings on these hydrogens result from interactions with the ring-carbon π-orbitals, which carry most of the unpaired spin. A maximum interaction (and hence maximum absolute value of the isotropic hfcc) will occur when a hydrogen lies perpendicular to the ring plane, whereas for a hydrogen lying in the plane of the ring, the isotropic hfcc will be very near zero. The values of the hfcc of the two β-protons will hence serve as a very sensitive probe of the relative orientation of the ring plane relative to the plane defined by the atoms C_1-C_β-C_α. In the symmetrical orientations (dihedral angle $\theta_{C_6\text{-}C_1\text{-}C_\beta\text{-}C_\alpha}$ set to 0° or 90°, respectively) that were used in the optimizations of the *p*-ethylphenoxyl radical as described above, the β-protons are equivalent in both cases. For the energetically lowest of these ($\theta = 90°$, Fig. 1 *c*), the isotropic components of the two β-protons are 4.4 G, and the anisotropies are very small.

We will in the following use two notations for the dihedral (rotational) angles: either dihedral θ_1 and θ_2 for the β-protons, or rotational θ for the α-carbon, as illustrated in Fig. 2. According to this definition the β-proton dihedral angles are 30° and 150° for $\theta = 0°$, and ±60° for $\theta = 90°$, respectively.

The hyperfine couplings of the β-protons, and hence the orientation of the side chain of the tyrosyl radical, have been determined to high accuracy for a number of different proteins (Barry et al., 1990; Bender et al., 1989; Hoganson and Babcock, 1992; Rigby et al., 1994) and are found to differ, depending on the radical environment. In particular, it has been concluded that the two protons are placed asymmetrically with respect to the plane of the ring for all different tyrosyl radicals observed so far. Hence our symmetrical models used in the geometry optimizations (cf. Fig. 1 *c*) are inappropriate in this respect. Rotating the ethyl group about the C_1-C_β bond, and comparing computed and experimental hfcc of the β-protons, we may use theory as a probe of the local geometry of tyrosyl radicals in different proteins, to complement available crystallographic data. This may serve to reveal the relative orientation of the amino acid side chain relative to the protein backbone.

The effect of ethyl group rotation on $A_{iso}(H)$ has previously been investigated by O'Malley and MacFarlane (1992) at the semiempirical AM1/INDO level of theory. They concluded that the ring protons are essentially unaffected by the rotation, but that the isotropic hfcc of the two β-protons fluctuate between 1 and 25 G as a result of the rotation. By comparing hfcc, very close agreement was found between the calculated rotational angles and those previously estimated from experiment on four different systems (Barry et al., 1990). The data available for, in particular, different RNR tyrosyl radicals, however, have been

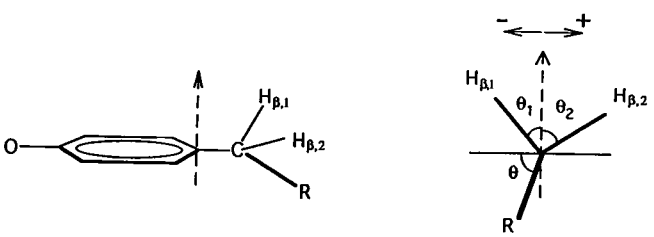

FIGURE 2 Definitions of the different dihedral angles used in describing the orientation of the β-protons (θ_1 and θ_2) and the α-carbon (θ). $\theta = 0°$ corresponds to placing the α-carbon in the plane of the ring, and when $\theta = 90°$ it is perpendicular to the ring.

complemented and updated considerably since then (see below).

In the present work we used the two PWP86/DZVP optimized conformers corresponding to 0° and 90° dihedral angles of the alkyl chain, and then performed single-point PWP86/IGLO-III calculations rotating in steps of 5°, adjusting the geometrical parameters linearly between the two end points (0° and 90°) at each step. The only geometrical parameter optimized in each step is the orientation of the terminal methyl group hydrogens, to reduce artificial effects of repulsion between the hydrogens and the atoms in the ring.

In Figs. 3 and 4 we show the results for the potential energy for the rotational motion, and for the corresponding hyperfine coupling constants of the two β-protons, respectively. In the latter we have used the notation A_{xx}, A_{yy}, and A_{zz} rather than the separate isotropic and dipolar components, for easy comparison with experimental data. The barrier to rotation (Fig. 3) is very low, less than 1 kcal/mol, and the global energy minimum is found at roughly 80° out-of-plane angle of C_α (angle θ in Fig. 2). We also note a local minimum at a dihedral angle θ of ~30°. The somewhat "jagged" structure of the potential energy curve is related to the limited geometry optimization performed for each rotational angle indicated. The large variation in the β-proton hyperfine parameters for these systems lies entirely in the isotropic hfcc, whereas the anisotropic components remain constant at (−0.7, −0.5, 1.2) ± 0.2 G for both protons. It should also be pointed out that the spin densities and hfcc on the remaining atoms are essentially unaffected by the ethyl group rotation.

The experimental hfcc for the two β-protons in the Y_z tyrosyl radical in PSII are (0.6, 0.4, 2.8) G and (10.4, 10.1, 12.6) G, respectively (Tommos et al., 1995). From Fig. 4 we can see that the best fit to the experimental data is obtained at a rotational angle $\theta = 75° \pm 5°$. This corresponds to dihedral angles θ_1 and θ_2 for the protons in question at 75° and −45°, respectively (cf. Fig. 2). This compares excellently with the dihedral angles derived from ENDOR data by Rigby et al. (1994) for the dark stable Y_D tyrosyl radical in Spinach PSII and in *C. reinhardtii* (dihedral angles (72.1°, −48.1°) and (72.7°, −47.4°), respectively), using the Stone-Maki relations. In an ESEEM study by Warncke et al. (1994), the values (1.85, 1.85, 5.09) G and (7.19, 7.19, 10.43) G were reported for the Y_D radical in the blue-green algae *Synechosystis* 6083. The dihedral angles were in that work determined to −52° and 68°, respectively. From our Fig. 4, the rotational angle θ corresponding to these experimental hyperfine parameters is 80° ± 5°, i.e., slightly larger than in the PSII systems studied by Rigby et al. The β-proton dihedrals are then −50° and 70°, again in very close correspondence with the empirically based estimates. For (thus far) one RNR system, in a normally nonexpressed RNR in *Salmonella typhimurium* (protein R2F in a class Ia RNR; Jordan et al., 1994), similar values for the β-protons have been obtained ((10.5, 9.5, 7.4) G for the large couplings and <3 G for the small couplings; Allard et al., 1996). These couplings would again correspond to a rotational angle of ~75°. This radical has been classified as an unusual, "relaxed" form (Allard et al., 1996) similar also to the isolated tyrosyl radicals in aqueous glass matrices (Hoganson et al., 1996).

The relative orientations of the "relaxed" tyrosyl radicals found in PSII and in *S. typhimurium* differ from those observed in RNR from mouse, herpes simplex, T4 bacteriophage, and *E. coli* bacteria (class Ia RNR). In these it has been concluded that the β couplings instead correspond to rotational angles of the α-carbon in the 20–40° range. In, e.g., *E. coli*, Bender et al. (1989) reported the values (21.6, 19.5, 20.6) G and (1.5, −0.7, −0.8) G, respectively. Similar

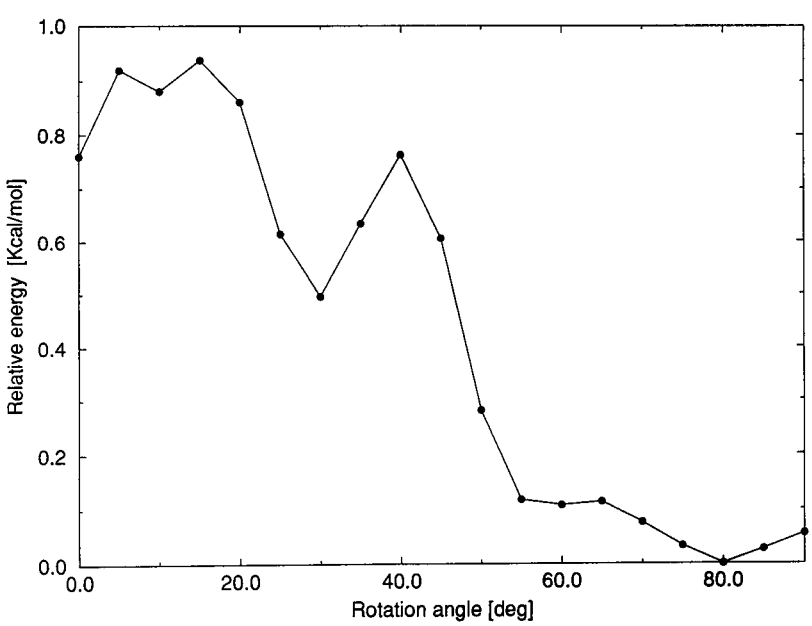

FIGURE 3 Relative energies of the *p*-ethylphenoxyl radical (Fig. 1 *c*), as function of rotational (dihedral) angle of the ethyl group. The geometries were fully optimized at the end points (θ = 0° and 90°), after which the structures for the remaining points were obtained by linearly varying between these two and reoptimizing the positions of the α-carbon protons.

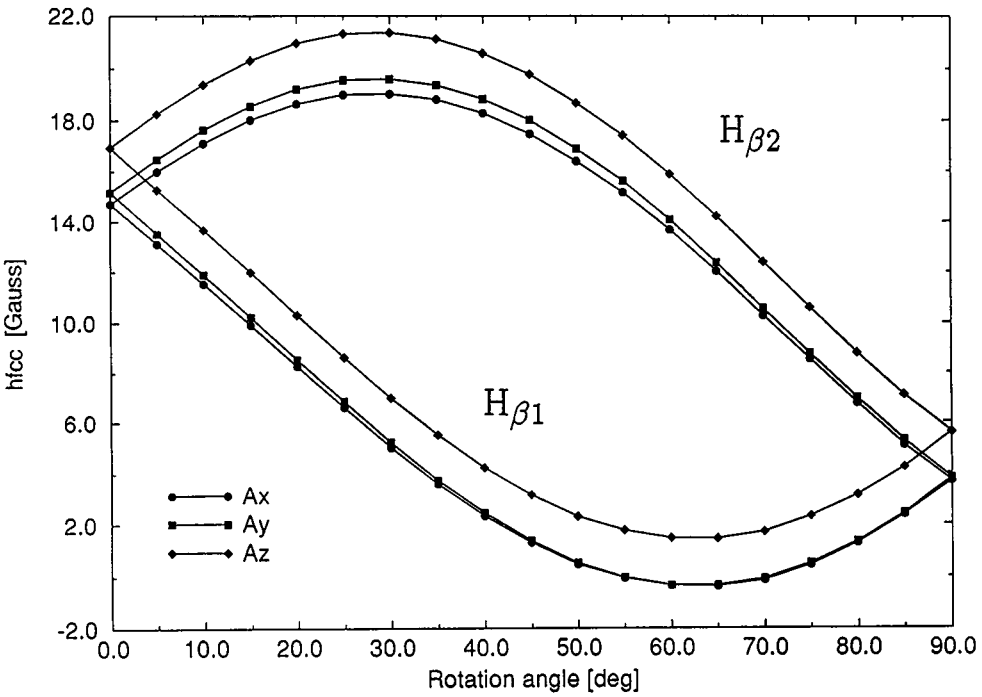

FIGURE 4 Effects of ethyl group rotation (cf. Figs. 2 and 3) on the hfcc of the β-protons in the *p*-ethylphenoxyl radical (Fig. 1 *c*). See text for experimental data of different tyrosyl radicals.

values were found by Hoganson and co-workers (1996), who also determined the oxygen hfcc and spin density as discussed above. The large couplings correspond to a rotational angle θ of 30 ± 5°, which is also the local energy minimum on the rotational potential surface (Fig. 3). For the couplings of the second methylene proton, Hoganson et al. discussed whether the isotropic component should be positive or negative. Based on the work of Bender et al., it was concluded that the contact interactions should be negative, leading to the very small couplings listed above. From Fig. 4 we note, however, that this would yield a rotational angle of ~60°—inconsistent with the θ = 30° rotational angle for the first methylene proton. From our study of the effects of rotating the ethyl group, and from the AM1/INDO study by O'Malley and MacFarlane (1992), we know, furthermore, that the isotropic hfcc of both β-protons remain positive throughout the rotational motion. Using a positive rather than a negative value for the contact interaction of the second methylene proton, the tensor components (3.8, 1.2, 1.4) G were derived (Hoganson et al., 1996). This would correspond to a rotational angle of 40–45°, much closer to the value determined for the first proton. Assuming a rotational angle θ of 35° as an average, the dihedral angles θ_1 and θ_2 for these two protons become ~−5 and +115°, respectively. In bacteriophage T4-induced RNR, the large hf coupling components were determined to be 19.6 G and 7.5 G, respectively (Sahlin et al., 1982). It was concluded that the hfcc should correspond to dihedral angles of about +10 and +130°, yielding a rotational angle θ of ~20°—relatively close to those of the previously discussed RNRs. We also note that the rotational angle of 10–30° for RNR tyrosyl radicals differs from the suggested 57–62° reported by O'Malley and MacFarlane (1992). In light of the present results and experimental data made available after 1992, however, a value of θ of ~20° appears more likely to be correct.

One tyrosyl radical system for which further studies seem required is that observed in prostaglandin H synthase (PGH). Originally this radical was concluded to have one large hyperfine component of 16 G (Kulmacz et al., 1990), a value that was later reevaluated to 19 G (Barry et al., 1990). The main hyperfine coupling of the second β-proton was deduced to be ~1 G. As seen from Fig. 4, the data set 16 and 1 G corresponds to a rotational angle of 60°, close to the previous estimates of 65°. At 19 G, however, we are in the 45° region, and appear to be at a local maximum on the energy surface (Fig. 3). Kulmacz et al. also reported a relaxed form of the radical, with the couplings 14 and 2 G. This corresponds to a rotational angle of ~70°, closer to the global minimum of Fig. 3.

From the above comparison, it seems clear that the present calculated values are of such accuracy that they can be used to determine very precisely the relative orientation between the phenyl ring and the alkyl chain. The preferred orientation of the tyrosyl radicals appears to fall into two classes, corresponding to values of θ of ~75° or ~30°. From our calculations, these values of the rotational angle also coincide with (local) minima on the rotational energy curve.

Also for β-protons, an empirical relation is frequently used to relate spin densitites to isotropic hfcc,

$$A_{iso}(H_{\beta n}) = B_0\rho + B_1\rho \cos^2\theta_n,$$

where θ_n is one of the β-hydrogen out-of-plane dihedral angles as defined in Fig. 2. Inserting our computed data of

hfcc and spin densities for different rotational angles, we obtain the values B_0 = 1.5 G and B_1 = 52.4 G at the PWP86/IGLO-III level. This agrees closely with the estimated values ≈0 and 58 G for B_0 and B_1, respectively, as derived by Bender et al. (1989).

Modeling hydrogen bonding

As noted above, hydrogen bonding is known to be present in, e.g., the Spinach PSII Y_D radical, but not in *E. coli* RNR (Hoganson et al., 1996). The presence of a hydrogen bond to the tyrosyl oxygen is believed to cause a reduction in oxygen spin density of ~10% (Hoganson et al., 1996). To see if we could model this effect theoretically, i.e., if hydrogen bonding really would result in such significant changes, a model was devised in which a nearby H-bonding group was modeled either as formic acid (HCOOH) or as water. These two compounds were first optimized at the PWP86/IGLO-III level, and then placed such that the oxygen in the water/formic acid (O′) was positioned according to data from a *g*-factor analysis by Un et al. (1995). From a comparison with crystallographic data for tyrosine hydrochloride (Fasanella and Gordy, 1969), the O_{Tyr}-O′ distance was determined to be 2.6 Å. Following the work by Un et al., we then used the parameters 150° for the C_4-O_{Tyr}-O′ bond angle and 40° for the O′-O_{Tyr}-C_4-C_5 dihedral angle. We kept the ethyl group at the 80° dihedral angle throughout, as described in the previous section. The two model systems are shown in Fig. 5. Initial studies showed that these two hydrogen bonding models generated potential energy surfaces and spin density distributions that were almost identical.

The effects on the spin density distribution due to the hydrogen bond are displayed in Table 4, where we list the

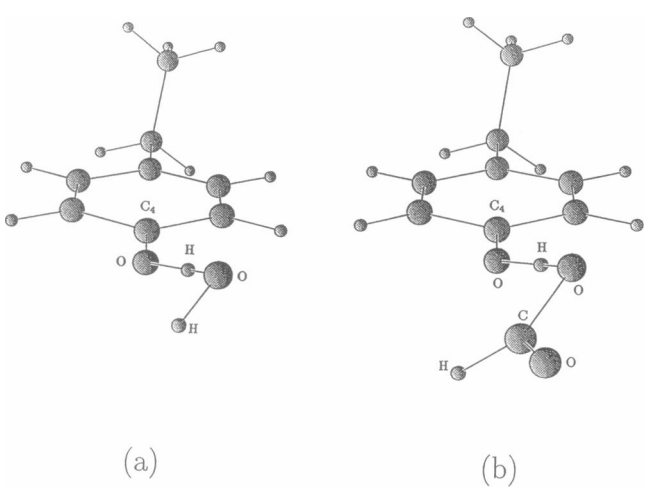

FIGURE 5 Models of hydrogen bonding to the tyrosyl radical. The H-bonding group is modeled by a water molecule (*a*) and by formic acid (*b*). The oxygen-oxygen distance is 2.6 Å, the C_4-O-O bond angle 150°, and the C_5-C_4-O-O dihedral angle 40°. The ethyl group is kept at the dihedral angle of 80°, corresponding to the energy minimum for ethyl group rotation.

TABLE 4 Spin densities of the *p*-ethylphenoxyl radical with the dihedral angle *θ* fixed at 80°

	Calculated		Experimental	
Atom	I	II	RNR	PSII
Cβ	−0.04	−0.03	0.03	0.01
C1	0.39	0.39	0.38	0.37
C2/C6	−0.12	−0.11	−0.08	−0.07
C3/C5	0.27	0.25	0.25	0.24
C4	−0.03	0.02	−0.05	0.01
O	0.37	0.32	0.29	0.26

Results are shown for the system without H bonding (I) and when H bonding is modeled with formic acid (II). Experimental data for *E. coli* RNR (no H bond) and spinach Y_D (H bond assumed present) (Hoganson et al., 1996) are also included. Note that the experimental values of the oxygen spin densities are based on empirical parameters derived from peroxide studies.

spin densities for the ethyl-substituted systems with and without H bonding (formic acid). We also include the experimental data for the corresponding compounds in which H bonding is absent (*E. coli* RNR) or present (spinach PSII). The experimental changes in spin density caused by the hydrogen bond on O and on C_4 are −0.03 and +0.06, respectively. From the present calculations we get the change −0.05/−0.06 (water/formic acid) on the oxygen, and +0.03/+0.05 on C_4, in very close agreement with the experimental observations. For the other atoms, the shifts in spin densities are hardly significant. We conclude that the change in spin density caused by hydrogen bonding is well reproduced with the present approach.

Finally, if we consider the calculated hyperfine coupling constants for the protons and the tyrosyl oxygen of these systems (no H bond, H bond to water, H bond to formic acid), we note that the hfcc are very similar for all three systems, although some small changes can be observed, even for the β-protons. Small differences in hfcc for the "equivalent" ring protons H2 and H6, and H3 and H5, as reported by O'Malley and co-workers (Rigby et al., 1994) for the Y_D radical in PSII, are already observed when a rotational angle for the α-carbon of 80° is used, without the presence of the H bond. A minor difference in the asymmetry is observed between the non-H-bonded and H-bonded models for these protons, with a better agreement for the H2/H6 pair in the H-bonded case, and for the H3/H5 pair for the system with no H bond. The Y_D radical is believed to be H-bonded. The main feature in the computed hfcc for the H-bonded system is, however, a 2–4 G reduction (absolute numbers) in anisotropic couplings on $^{17}O_{Tyr}$, and the presence of anisotropic couplings by the same amount on the proton involved in the H-bonding. The isotropic coupling of the H-bonding proton is rather small: −0.8 G for the water system and −0.3 G for the formic acid model. We stress, however, that the present study of H bonding is a model, and that the exact position of the H-bonding moiety has not been fully geometry-optimized in the present work.

CONCLUSIONS

We have in the present work, as a first study in a series of amino acid radicals, applied gradient-corrected DFT (PWP86) to calculate geometrical structures, spin density distributions, and hyperfine properties of a set of model tyrosyl radicals. The tyrosyl radical systems are among the most studied experimentally, and we can hence use the available data as a "calibration" for the suggested theoretical approach. Initially four models of tyrosyl radicals were tested, three neutral and one positively charged. We could confirm that the spin density distributions and proton hyperfine couplings of the neutral phenoxyl radicals were in much closer overall agreement with experimental data than the corresponding data for the radical cation. We also showed that the effects of alkyl substitution to the ring (i.e., modeling the link between the phenoxyl group and the protein backbone) on the distribution of the unpaired electron were very minor. Based on data for ^{17}O-labeled tyrosine radicals in *E. coli* RNR (Hoganson et al., 1996), we suggest a revision of the empirical parameters used to deduce the total hyperfine tensor and the experimental oxygen spin density. The agreement between theory and experiment, once the revised parameters are employed, is most satisfactory. For the ring protons it is concluded that different empirical parameters should be employed for the protons closer to the oxygen (Q(H3/H5) $\simeq -22$ G) compared to those further away (Q(H2/H6) $\simeq -12$ G), contrary to previous estimates. Whether this discrepancy is related to problems with the McConnell relation or with the computed spin densities of the present work is not entirely resolved.

As a second step, we rotated the ethyl group in the *p*-ethylphenoxyl radical, to investigate the effects of the local geometry on the hyperfine couplings of the two β-protons. A local minimum was observed at a $\sim 30°$ out-of-plane angle, whereas the global minimum of the rotational potential curve was found at a $\sim 80°$ rotational angle. The potential energy surface in the area between 55° and 90° rotational angles was furthermore found to be very shallow (within 0.1 kcal/mol), and it is probable that the phenoxyl ring will undergo vibrational motion, leading to some averaging of the hyperfine parameters, unless stabilized through long-range H bonding or by "steric hindrance" caused by the presence of other amino acid side chains. The hfcc computed for the β-protons at a rotational angle θ of $75° \pm 5°$ (i.e., very close to the minimum on the potential energy curve) are found to agree excellently with observed experimental data for the "relaxed" tyrosyl radicals found in *S. typhimurium* RNR and in PSII. This value for the rotational angle agrees very well with previous data based on the empirical model by Stone and Maki (Rigby et al., 1994; Tommos et al., 1995), and with previous studies at the semiempirical AM1/INDO level (O'Malley and MacFarlane, 1992). For tyrosyl radicals found in other RNR systems (mouse, herpes simplex virus, *E. coli*, T4 bacteriophage) (Hoganson et al., 1996; Sahlin et al., 1982), the observed hfcc correspond to a rotational angle of 20–40°, indicating that this particular set of radicals is located close to the local minimum on the rotational potential surface. The corresponding dihedral angles for the two β-protons perfectly match those estimated in the experimental papers. The empirical parameters employed to estimate carbon spin densities from β-proton hfcc are tested and found to be in good agreement with the computed ones (B_0: calc. 1.4 G, est. 0; B_1: calc. 52.4 G, est. 58 G).

We finally investigated the effects on the spin density distributions caused by hydrogen bonding. Based on the geometric parameters for the location of the H-bonding group, determined by Un et al. (1995), two models were constructed in which we placed the H-bonding moiety (water or formic acid) at a 40° out-of-plane angle. The oxygens involved in the H bond were positioned 2.6 Å apart, and with a C_4-O_{Tyr}-O bond angle equal to 150°. The two model systems were found to generate almost identical results—a reduction in spin density on the tyrosyl oxygen by 0.05–0.06 and an increase on C_4 by 0.03–0.05. This should be compared with the differences observed for different proteins believed to lack/have H bonding to the tyrosyl radical oxygen: -0.03 for O and $+0.05$ for C_4 (Hoganson et al., 1996).

To summarize, the present approach (PWP86/DZVP optimizations followed by PWP86/IGLO-III single-point calculations for energetics and hyperfine properties) appears to be highly accurate in describing the intricate details observed for the tyrosyl radicals in, e.g., photosystem II and ribonucleotide reductases. Aspects such as the nature of the radical (neutral/charged), conformational effects on hyperfine properties of the β-protons, and subtle hydrogen bonding interactions are found to be well reproduced.

We thank Drs. Hoganson, Sahlin, Sjöberg, and Babcock for making their manuscript (Hoganson et al., 1996) available before publication.

The Swedish Natural Science Research Council (NFR) is gratefully acknowledged for financial support.

REFERENCES

Allard, P., A. L. Barra, K. K. Andersson, P. P. Schmidt, M. Atta, and A. Gräslund. 1996. Characterization of a new tyrosyl free radical in *Salmonella typhimurium* ribonucleotide reductase with EPR at 9.45 and 245 GHz. *J. Am. Chem. Soc.* 118:895–897.

Andzelm, J., and E. Wimmer. 1992. Density functional Gaussian-type orbital approach to molecular geometries, vibrations and reaction energies. *J. Chem. Phys.* 96:1280–1303.

Babcock, B. T., M. K. El-Deeb, P. O. Sandusky, M. M. Whittaker, and J. W. Whittaker. 1992. Electron paramagnetic resonance and electron nuclear double resonance spectroscopies of the radical site in galactose oxidase and of thioether-substituted phenol model compounds. *J. Am. Chem. Soc.* 114:3727–3734.

Barone, V. 1994. Inclusion of Hartree-Fock exchange in density functional methods. Hyperfine structure of second row atoms and hydrides. *J. Chem. Phys.* 101:6834–6838.

Barone, V. 1996. Structure, magnetic properties and reactivities of open-shell species from density functional and self-consistent hybrid methods. *In* Recent Advances in Computational Chemistry, Vol. 1, Part I. D. P. Chong, editor. World Scientific, Singapore. 287–334.

Barry, B. E., and G. T. Babcock. 1987. Tyrosine radicals are involved in the photosynthetic oxygen evolving system. *Proc. Natl. Acad. Sci. USA.* 84:7099–7103.

Barry, B. E., M. K. El-Deeb, P. O. Sandusky, and G. T. Babcock. 1990. Tyrosine radicals in photosystem II and related model compounds. *J. Biol. Chem.* 265:20139–20143.

Bauschlicher, C. W., Jr. 1995. A comparison of the accuracy of different functionals. *Chem. Phys. Lett.* 246:40–44.

Becke, A. D. 1993. A new mixing of Hartree-Fock and local density functional theories. *J. Chem. Phys.* 98:1372–1377.

Bender, C. J., M. Sahlin, G. T. Babcock, B. A. Barry, T. K. Chandrashekar, S. P. Salowe, J. Stubbe, B. Lindström, A. Ehrenberg, and B.-M. Sjöberg. 1989. An ENDOR study of the tyrosyl free radical in ribonucleotide reductase from *Escherichia coli*. *J. Am. Chem. Soc.* 111:8076–8083.

Broze, M., Z. Luz, and B. J. Silver. 1967. Oxygen-17 hyperfine splitting constants in the ESR spectra of *p*-semiquinones-^{17}O. *J. Chem. Phys.* 46:4891–4902.

Chipman, D. M., R. Liu, X. Zhou, and P. Pulay. 1994. Structure and fundamental vibrations of phenoxyl radical. *J. Chem. Phys.* 100: 5023–5035.

Cohen, M. J., and D. P. Chong. 1995. Density functional calculations of Fermi contact hyperfine coupling parameters. *Chem. Phys. Lett.* 234: 405–412.

Daul, C., A. Goursot, and D. R. Salahub. 1993. Numerical calculation of multicentre integrals for polyatomic molecules. *In* Numerical Grid Methods and Their Application to Schrödinger's Equation, C. Cerjan, editor, NATO ASI C412. 153–174.

Dixon, W. T., and D. Murphy. 1972. Determination of the acidity constants of some phenol radical cations by means of electron spin resonance. *J. Chem. Soc. Faraday Trans II.* 72:1221–1230.

Dixon, W. T., and R. Norman. 1964. Electron spin resonance studies of oxidation. Part IV. Some benzenoid compounds. *J. Chem. Soc.* 4857–4860.

Eriksson, L. A. 1995. Accurate density functional theory calculations of cationic magnesium clusters and Mg^+-rare gas interactions. *J. Chem. Phys.* 103:1050–1056.

Eriksson, L. A., O. L. Malkina, V. G. Malkin, and D. R. Salahub. 1994. The hyperfine structures of small radicals from density functional calculations. *J. Chem. Phys.* 100:5066–5075.

Eriksson, L. A., J. Wang, and R. J. Boyd. 1995. The interactions between alkali metals and C_2H_2: density functional theory as an analytical tool. *Chem. Phys. Lett.* 235:422–429.

Fasanella, E. L., and W. Gordy. 1969. Electron spin resonance of an irradiated single crystal of L-tyrosine-HCl. *Proc. Natl. Acad. Sci. USA.* 62:299–304.

Godbout, N., D. R. Salahub, J. Andzelm, and E. Wimmer. 1992. Optimization of Gaussian-type basis sets for local spin density functional calculations. Part I. Boron through neon, optimization technique and validation. *Can. J. Chem.* 70:560–571.

Gräslund, A., and M. Sahlin. 1996. Electron paramagnetic resonance and nuclear magnetic resonance studies of class I ribonucleotide reductase. *Annu. Rev. Biophys. Biophys. Chem.* 25:259–286.

Hoganson, C. W., and G. T. Babcock. 1992. Protein-tyrosyl radical interactions in photosystem II studied by electron spin resonance and electron nuclear double resonance spectroscopy: comparison with ribonucleotide reductase and in vitro tyrosine. *Biochemistry.* 31:11874–11880.

Hoganson, C. W., M. Sahlin, B.-M. Sjöberg, and G. T. Babcock. 1996. Electron magnetic resonance of the tyrosyl radical in ribonucleotide reductase from *Escherichia coli*. *J. Am. Chem. Soc.* 118:4672–4679.

Hohenberg, P., and W. Kohn. 1964. Inhomogeneous electron gas. *Phys. Rev.* B136:864–871.

Huzinaga, S. 1965. Gaussian-type functions for polatomic systems, I. *J. Chem. Phys.* 42:1293–1302.

Huzinaga, S., and Y. Sakai. 1969. Gaussian-type functions for polatomic systems, II. *J. Chem. Phys.* 50:1371–1381.

Johnson, B. G., P. W. M. Gill, and J. A. Pople. 1993. The performance of a family of density functional methods. *J. Chem. Phys.* 98:5612–5626.

Jordan, A., E. Pontis, M. Atta, M. Krook, I. Gibert, J. Barbé, and P. Reichard. 1994. A second class I ribonucleotide reductase in Enterobacteriaceae: characterization of the *Salmonella typhimurium* enzyme. *Proc. Natl. Acad. Sci. USA.* 91:12892–12896.

Kohn, W., and L. J. Sham. 1965. Self-consistent equations including exchange and correlation effects. *Phys. Rev.* A140:1133–1138.

Kulmacz, R. J., Y. Ren, A.-L. Tsai, and G. Palmer. 1990. Prostaglandin H synthase: spectroscopic studies of the interaction with hydroperoxides and with indomethacin. *Biochemistry.* 29:8760–8771.

Kutzelnigg, W., U. Fleischer, and M. Schindler. 1990. NMR—Basic Principles and Progress, Vol. 23. Springer-Verlag, Heidelberg.

Lee, C., W. Yang, and R. G. Parr. 1988. Development of the Colle-Salvetti correlation-energy formula into a functional of the electron density. *Phys. Rev.* B37:785–789.

Liu, R., and X. Zhou. 1993. Structures of PhX (X = O and N). Importance of polarization functions in the basis set. *Chem. Phys. Lett.* 207:185–189.

Malkin, V. G., O. L. Malkina, L. A. Eriksson, and D. R. Salahub. 1995. The calculation of NMR and ESR parameters using density functional theory. *In* Theoretical and Computational Chemistry, Vol. 2: Modern Density Functional Theory: A Tool for Chemistry. P. Politzer and J. M. Seminario, editors. Elsevier, Amsterdam. 273–334.

McConnell, H. M., and J. Strathdee. 1959. Theory of anisotropic hyperfine interactions in π-electron radicals. *Mol. Phys.* 2:129–138.

Neta, P., and R. W. Fessenden. 1974. Hydroxyl radical reactions with phenols and anilines as studied by electron spin resonance. *J. Phys. Chem.* 78:523–529.

Nordlund, P., and H. Eklund. 1993. Structure and function of the *Escherichia coli* ribonucleotide reductase protein R2. *J. Mol. Biol.* 232: 123–164.

Nordlund, P., B.-M. Sjöberg, and H. Eklund. 1990. Three-dimensional structure of the free radical protein of ribonucleotide reductase. *Nature.* 345:593–598.

O'Malley, P. J., and A. J. MacFarlane. 1992. Calculated proton hyperfine coupling values for the tyrosine radical using an AM1/INDO method. *J. Mol. Struct. (Theochem.).* 277:293–297.

O'Malley, P. J., A. J. MacFarlane, S. E. J. Rigby, and J. H. A. Nugent. 1995. The geometry and spin density distribution of the tyrosyl radical: a molecular orbital study. *Biochim. Biophys. Acta.* 1232:175–179.

Parr, R. G., and W. Yang. 1989. Density Functional Theory of Atoms and Molecules. Oxford University Press, New York.

Perdew, J. P. 1986a. density-functional approximation for the correlation energy of the inhomogeneous electron gas. *Phys. Rev.* B33:8822–8824.

Perdew, J. P. 1986b. Erratum: density-functional approximation for the correlation energy of the inhomogeneous electron gas. *Phys. Rev.* B34: 7406.

Perdew, J. P., and Y. Wang. 1986. Accurate and simple density functional for the electronic exchange energy: generalized gradient approximation. *Phys. Rev.* B33:8800–8802.

Qin, Y., and R. A. Wheeler. 1995a. Similarities and differences between phenoxyl and tyrosine phenoxyl radical structures, vibrational frequencies and spin densities. *J. Am. Chem. Soc.* 117:6083–6092.

Qin, Y., and R. A. Wheeler. 1995b. Density-functional methods give accurate vibrational frequencies and spin densities for phenoxyl radical. *J. Chem. Phys.* 102:1689–1698.

Qin, Y., and R. A. Wheeler. 1996. Density-functional-derived structures, spin properties, and vibrations for phenol radical cation. *J. Phys. Chem.* 100:10554–10563.

Rigby, S. E. J., J. H. A. Nugent, and P. J. O'Malley. 1994. The dark stable tyrosine radical of photosystem 2 studied in three species using ENDOR and EPR spectroscopies. *Biochemistry.* 33:1734–1742.

Sahlin, M., A. Gräslund, A. Ehrenberg, and B.-M. Sjöberg. 1982. Structure of the tyrosyl radical in bacteriophage T4-induced ribonucleotide reductase. *J. Biol. Chem.* 257:366–369.

Salahub, D. R., R. Fournier, P. Mlynarski, I. Papai, A. St-Amant, and J. Ushio. 1991. Gaussian-based density functional methodology, software, and applications. *In* Density Functional Methods in Chemistry. J. Labanowski and J. Andzelm, editors. Springer, New York. 77–100.

Sevilla, M. D., D. Becker, and M. Yan. 1990. Structure and reactivity of peroxyl and sulphoxyl radicals from measurement of oxygen-17 hyperfine couplings: relationships with Taft substituent parameters. *J. Chem. Soc. Faraday Trans.* 86:3279–3286.

Sim, F., D. R. Salahub, S. Chin, and M. Dupuis. 1991. Gaussian density functional calculations on the allyl and polyene radicals: C_3H_5 to $C_{11}H_{13}$. *J. Chem. Phys.* 95:4317–4326.

St-Amant, A. 1991. Ph.D. thesis. Université de Montréal.

St-Amant, A., and D. R. Salahub. 1990. New algorithm for the optimization of geometries in local density functional theory. *Chem. Phys. Lett.* 169:387–392.

Stone, E. W., and A. H. Maki. 1962. Hindered internal rotation and ESR spectroscopy. *J. Chem. Phys.* 37:1326–1333.

Tommos, C., X.-S. Tang, K. Warncke, C. W. Hoganson, S. Styring, J. McCracken, B. A. Diner, and G. T. Babcock. 1995. Spin-density distribution, conformation, and hydrogen bonding of the redox-active tyrosine Y_z in photosystem II from multiple electron magnetic resonance spectroscopies: implications for photosynthetic oxygen evolution. *J. Am. Chem. Soc.* 117:10325–10335.

Un, S., M. Atta, M. Fontecave, and A. W. Rutherford. 1995. *g*-values as a probe of the local protein environment: high-field EPR of tyrosyl radicals in ribonucleotide reductase and photosystem II. *J. Am. Chem. Soc.* 117:10713–10719.

Warncke, K., G. T. Babcock, and J. McCracken. 1994. Structure of the Y_D tyrosine radical in photosystem II as revealed by ^2H electron spin echo interactions. *J. Am. Chem. Soc.* 116:7332–7340.